Advances in Science and Technology Research Journal

Advances in Science and Technology Research Journal, 2027, 21(1), 379–392
https://doi.org/10.12913/22998624/235904
ISSN 2299-8624, License CC-BY 4.0

Received: 2026.08.07
Accepted: 2026.11.15
Published: 2026.12.01

Microstructure, hardness, and porosity of porous composite brass prepared by the powder metallurgy route

Ruaa Hatem Kadhim[1*], Shahad Ali Hammood[1], Haydar Al-Ethari[1]

[1] Department of Metallurgical Engineering, College of Materials Engineering, University of Babylon, 51001 Hillah, Babil, Iraq
* Corresponding author's e-mail: ruaa.hatem@uobabylon.edu.iq

ABSTRACT

This work aimed to prepare a porous brass composite material reinforced with boron carbide and select the optimal conditions to achieve the highest porosity with the highest possible hardness. Samples were prepared using the powder metallurgy technique. Brass (70% Cu, 30% Zn) was reinforced with 3, 6, and 9 Wt.% of boron carbide. To create the pores, spherical urea granules (diameter approximately 425 µm) were used as a space holder at a weight percentage of 30%. The purity of urea was 99.5%. After the compaction process, the urea was removed using hot water at 100 degrees Celsius. The powders were compacted at three different pressures: 600, 700, and 800 MPa. The specimens were sintered at temperatures of 650, 700, and 750 °C for 120 min under a vacuum atmosphere of 10^{-4} tor. Taguchi method (L_9) in Minitab 18 was used to design the experimental part. The results showed apparent porosity of 22% to 34% and microhardness of 238 HV to 302 HV. The microstructure exhibited a comparatively homogeneous dispersion of B_4C particles in the brass matrix while maintaining the porous structure resulting from urea removal. The results also indicated that increasing the compacting pressure and sintering temperature, as well as the weight percentage of B_4C, led to improved densification, reduced porosity, and increased hardness. These results suggest that controlling manufacturing parameters is essential for enhancing the properties of porous brass composites and producing materials with improved mechanical performance. The results of the experiments were analysed using analysis of variance, and the response surface methodology and the desirability function analysis were used to determine the optimal conditions. The optimisation results showed a good value for composite desirability, indicating good agreement between the studied responses.

Keywords: brass- boron carbide, powder metallurgy, urea, pores (space holder), porous composite materials.

INTRODUCTION

Metallic materials with purposefully produced pores in their structure are known as porous metals. They therefore have a particularly favourable mix of mechanical and physical characteristics due to their unique structure, including an extremely low specific weight, an excellent rigidity-to-weight ratio, sound absorption capacity, and other properties [1,2]. Powder metallurgy is a solid-state manufacturing technique. This process produces metal composite materials by mixing metal powders and pressing them together to form a compact body. Then, the sintering process takes place at a suitable temperature, depending on the type of material to be produced, to form bonds between the powder particles as well as develop the final structure and properties of the material [3]. This technology allows for the manufacture of alloys and composites without the need to melt their components completely, as it allows control over the composition, microstructure, and properties by controlling the manufacturing conditions (pressing, sintering). Techniques such as hot pressing and sintering have been used in the production of metal alloys and composites. Studies have shown that changing the manufacturing conditions, as well as the type and proportion of the reinforcing material, directly affects the microstructure and properties of the produced

material [4–6]. The porous materials fabricated using powder Metallurgy techniques are rapidly advancing to fulfil a wide variety of new applications. Porous materials are usually sintered to densities ranging from 25% to 85% of the theoretical mean density. Filtration systems, fluid flow control, self-lubricating bearings, and medicinal applications are just a few of the specialised goods made from these specially developed materials [7, 8]. Brass (Cu–Zn alloy) is frequently utilised in engineering applications due to its corrosion resistance and mechanical properties, and ease of fabrication by powder metallurgy. Low hardness in some brass alloys prevents their use in the applications that need high mechanical properties [9, 10]. This led researchers to develop brass-based composite materials by reinforcing with high-hardness particles such as boron carbide (B_4C), silicon carbide (SiC), and other ceramic particles to improve mechanical properties without significantly altering other properties [11, 12]. Boron carbide is one of the most important reinforcing materials utilised in metal-based composites because of its superior qualities, such as high hardness and low density, high modulus of elasticity, and corrosion resistance, among others [13]. These properties make B_4C an effective material for improving mechanical performance without a significant increase in weight [14].

Studies have shown the powder metallurgy route to be one of the most suitable methods for producing porous materials using space holder techniques, as it provides control of the pores, their shape, and distribution. Controlling the type of space holders and the compacting and sintering conditions directly affects the final product [15,16]. Urea is widely used as a pore preservative because of its low cost, ease of mixing with mineral powders, and the possibility of removing it by dissolving it in water before the sintering process, where interconnected pores are formed [17].

Many researchers in recent years have focused on manufacturing porous metals using PM techniques. Contreras et al. [18] demonstrated that using a space holder technique provides an effective way to control pore size and shape. Water-soluble materials such as urea are among the most suitable for producing porous structures. Manohar et al. [19] also addressed the fabrication of metal composites reinforced with B_4C particles, noting that the addition of B_4C increases hardness and improves strength. In a recent study, Xiao et al. [20] studied the effects of the shape of the pore-preserving material on porous copper, and the results showed that the form and dimensions of the material directly affect the form of the pores, their degree of bonding, and their mechanical properties.

In previous studies, various materials such as sodium chloride, ammonium bicarbonate, polymethyl methacrylate, and urea were used as space holders in the manufacture of porous minerals. The importance of porous minerals is highlighted in many applications, such as filters, self-lubricating bearings, heat exchangers, energy absorbers, sound insulators, and biomedical applications. Fujii et al. [21] used sodium chloride (NaCl) to produce pores, as it is one of the most commonly used materials due to its ease of solubility in water. Lascano et al. [22] used ammonium bicarbonate (NH_4HCO_3) in the manufacture of porous metals, where it decomposes thermally at low temperatures and is used especially with titanium and magnesium. Aydoğmuş et al. [23] produced porous $Ti_{74}Nb_{26}$ alloys utilising Mg particles as a space holder combined with hot pressing and sintering, producing porosity values ranging from 45% to 68%. The study showed that porosity had major effects on the mechanical characteristics of the alloys that were created. Lee et al. [24] used polymethyl methacrylate (PMMA) to produce controlled pores, which decomposes thermally. The selection of these materials depends on their solubility, stability during compression, and their effect on the size and shape of the resulting pores. Sharma et al. [25] used urea as a pore component and investigated its effect on titanium foam. Another study by Sharma et al. [26] utilised spherical urea granules to produce stainless steel foam. Čaplovičová et al. [27] used urea to produce biodegradable porous iron, studying the effect of urea content on structure, porosity, and corrosion rate. Urea has garnered increasing attention in recent years due to its ease of solubility in water, low cost, and availability in various sizes and shapes, which allows for control over the resulting porosity. He et al. [28] studied the fabrication of a porous material using urea with a copper matrix. He focused on the effect of the size of the urea forming the pores on the final porosity of the material. Also, Xiao et al. [20] studied porous copper materials with added urea as a pore-forming material, focusing on the effect of the shape of the urea (spherical, acuminate) on the porous structure and mechanical properties. Moradi et al. [29] investigated the production of a boron carbide-reinforced metal foam using an

aluminium matrix. Therefore, urea was chosen in this study because of its ease of dissolution and the possibility of obtaining a homogeneous porous structure while maintaining the integrity of the metal matrix after sintering. According to available studies, porous metallic materials have been produced from aluminium, titanium, and steel, as well as copper and aluminium reinforced with boron carbide. However, brass reinforced with boron carbide, the use of urea as a pore-forming agent, and the effect of manufacturing conditions such as sintering temperature, compression pressure, and addition ratio have not been studied. In addition, the application of Taguchi and ANOVA analyses improves the manufacturing conditions and evaluates the effect of their variables. This represents the scientific novelty of the current study. Table 1 shows the research gap between the previous studies and the current study. Therefore, this research aimed to fabricate such composites and study the influence of B_4C content, compacting pressure, and sintering temperature on their microstructure, apparent porosity, and microhardness. Taguchi method (L9) in Minitab 18 was used to design the experimental part. The results were analysed, and the response surface methodology (RSM) and the desirability function analysis (DFA) were used to reach the optimal condition.

EXPERIMENTAL PART

The materials used

The materials utilised in this investigation were powders of brass (70% Cu, 30% Zn) and boron carbide (B_4C), as well as urea granules ($CO(NH_2)_2$) as a space holder to create porosity after dissolution and prepare a porous composite material. Chemical composition and particle size analysis were performed on the materials used in this study. Table 2 displays the purity, particle size, particle shape, and density of these powders.

Experimental design

In this work, the Taguchi method (L9) in Minitab 18 was used to design the experimental part and three planes for three variables: compacting pressure (600, 700, and 800 MPa), B_4C content (3, 6, and 9 wt.%), and sintering temperature (650, 700, and 750 °C). These ranges of parameters were selected based on previous studies related to the manufacture of metal composite materials by powder metallurgy, taking into account the nature of the materials used and the requirements for manufacturing the porous composite in the current study. This method allows for determining the effect of different conditions to obtain the best properties.

Table 1. Comparison between the present study and available studies related to porous materials that used Urea as a space holder

(Reference)	(Matrix)	(Reinforcement)	(Space holder)	(Manufacturing method)	(Research focus)
Hi Y. et al. [28]	Copper (Cu)	None	Carbamide = Urea	Powder metallurgy	The effect of the size of the pore-forming material on the pore structure and mechanical properties of porous copper.
Xiao et al. [20]	Copper (Cu)	None	Carbamide	Powder metallurgy	The effect of the shape of the pore-forming material on the pore structure and mechanical properties of porous copper.
Čákyová V. et al. [27]	Iron (Fe)	None	Urea	Powder metallurgy	Studying the porous structure and its properties to use them in medical applications.
Jain et al. [26]	Stainless steel (SS)	None	Urea	Powder metallurgy	Study the microstructure and compressive deformation behaviour of stainless-steel foam using urea as a space holder.
Moradi et al. [29]	Aluminium (Al)	B_4C	Carbamide	Powder metallurgy	Characterisation of porous Al–B_4C composites and evaluation of their pore characteristics and mechanical properties.
Present study	Brass	B_4C	Urea	Powder metallurgy + Taguchi + ANOVA	Development and optimisation of porous brass–B_4C composites by optimising processing parameters to achieve a desirable balance between porosity and microhardness.

Table 2. The details of materials used in this work

Materials	Purity	Avg. particle size(μm)	Particle shape	Density (g/cm³)	Source
Brass powder	99.5	45–65	Irregular	8.52	Chengdu Jinchun Metallic Materials Co., Ltd., China
Boron carbide B_4C	99.32	10–16	Irregular	2.93	Xi'an Function Material Group Co. Ltd., Xi'an, Shaanxi, China
Urea (placeholder)	99.0	400–600	Granular/Nearly spherical	1.52	Alpha Chemika, India

Samples preparation

The samples were prepared by mixing brass powder with a weight percentage of B_4C (3, 6, and 9 wt.%) and a constant percentage of urea (about 30%) to prepare a porous composite material. The wet mixing process with 2% acetone was achieved using the electric mixture type STGQM-15 / -2 for approximately 2 hrs. to achieve a smooth and homogeneous distribution of the powder particles. Disk specimens with a diameter of 15 mm and a height of 3 mm were prepared using a specially designed steel die. The compacting process was performed on an electric-hydraulic press, type CT340-CT440. The internal walls of the steel die were greased with graphite. All compacting processes were carried out at a constant loading rate of 0.3 kN/Sec. The pressures were 600, 700, and 800 MPa. The urea was removed from the green compact by dissolving it in hot water at 100 °C. After that, the green compacts were placed in the ultrasonic cleaner device, type VGT-1860QTD-42 kHz, for 30 min to ensure that each urea particle was removed. Then, the green compact was dried in the furnace at 100 °C before sintering. The green compacts were sintered in a vacuum tube furnace, type GSL 1600X, including heating for about 1 hour at 200 °C and then at temperatures of 650 °C, 700 °C, and 750 °C for 2 hours. Slow cooling in the furnace with a continuing vacuum to room temperature was performed. The process of sintering is shown in Figure 1. The illustration of the overall sample preparation is shown in Figure 2.

Characterisation

Figure 3 shows sintered samples (15 mm diameter and 3 mm height). SiC paper grits were used to grind the specimens (180, 240, 400, 600, 800, 1000, 1200, and 2000); then, a diamond suspension was used to polish them. The specimens were etched with 5 g $FeCl_3$, 10 mL HCl, and 100 mL water at room temperature [30]. After etching, the specimens were washed with distilled water and dried in an electric dryer. An optical microscope, type 1280 XEQMM300TUSB, was used to capture the microstructure of the specimens. The porosity of the specimens was measured by Equation 1 according to ASTM B-328 [31]:

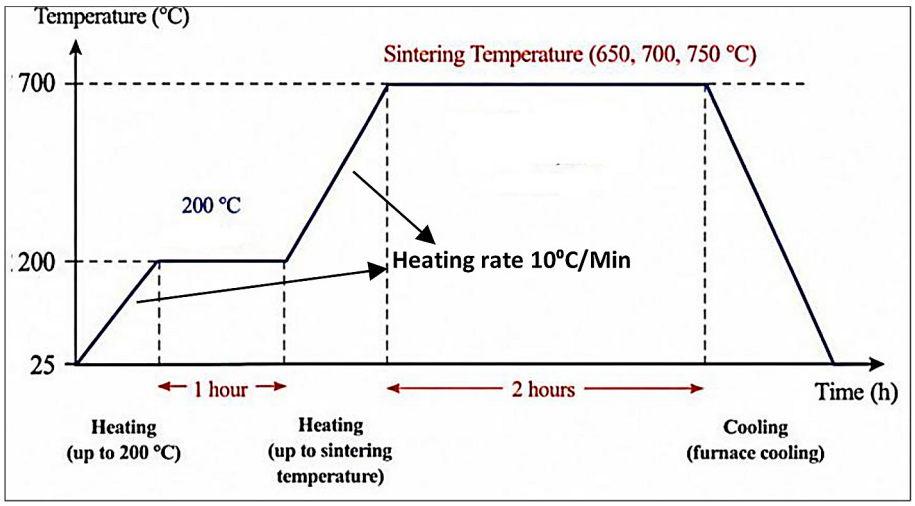


Figure 1. The green samples' sintering program

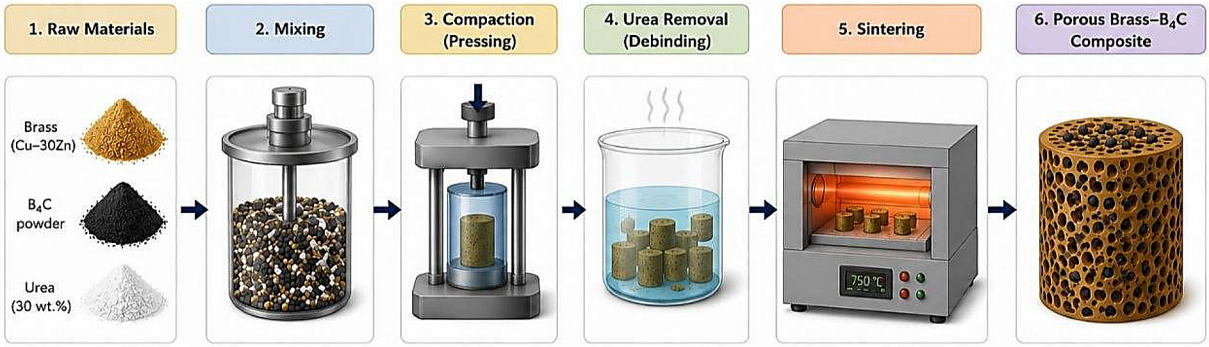


Figure 2. The schematic illustration was prepared based on the experimental procedure used in this study for the overall sample preparation

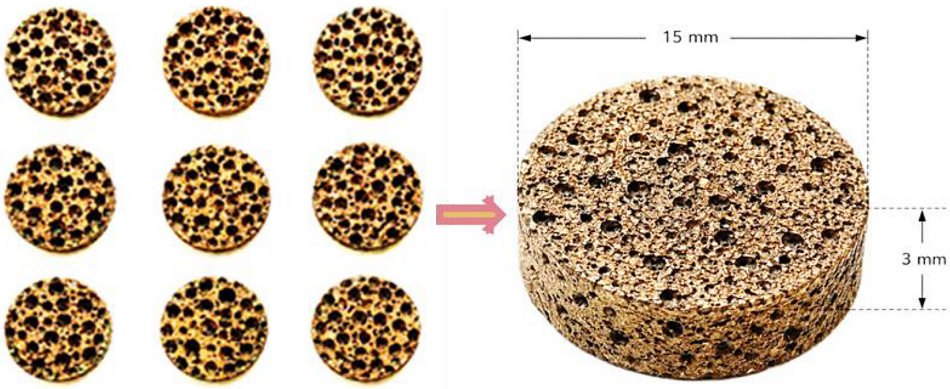


Figure 3. Samples of the prepared porous composite

$$Porosity\ (apparent)\% = \frac{Ww - Wd}{Wset - Ws} \times 100 \quad (1)$$

where: *Wd* is the specimen's dry weight (g), *Ww* is the specimen's wet weight (weighted following a 24-h immersion in distilled water) (g), *Wset* is the saturated weight (the sample was weighed after being submerged in distilled water at 80 °C for 5 h) (g), and *Ws* represents the suspended weight (weight of the sample). suspended in distilled water) (g).

Micro-Vickers hardness was used to measure the hardness of the sintered samples; a load of 50 g for 10 sec with a square-base diamond pyramid was used. The hardness was recorded as an average of five readings for each specimen.

RESULTS AND DISCUSSION

Microstructure results

Figure 4 represents the microstructure using optical microscopy of selected porous brass composites (S1, S5, S8). The B_4C particles, brass matrix, pores, and agglomeration are shown in the figure. These were determined based on the standard preparation of the samples, colour variation, morphological variation, and the known composition of the prepared samples. Therefore, the base region was attributed to the brass matrix, the lighter regions distributed within the matrix to B_4C particles, and the darker regions to pores resulting from urea removal. In addition, the B_4C particles that were close together were interpreted as agglomeration, based on their morphological characteristics and their distribution within the microstructure. The microstructure results showed that different proportions of the reinforcing material greatly affect its distribution within the matrix. The varying proportions of boron carbide led to variations in homogeneity, porosity, and bonding between the reinforcing material and the substrate. The homogeneous distribution is one of the most important factors affecting mechanical properties.

When a composite material is subjected to mechanical stresses, the applied load is transferred from the reinforcing particles to the substrate if the bonding is good, thus reducing the

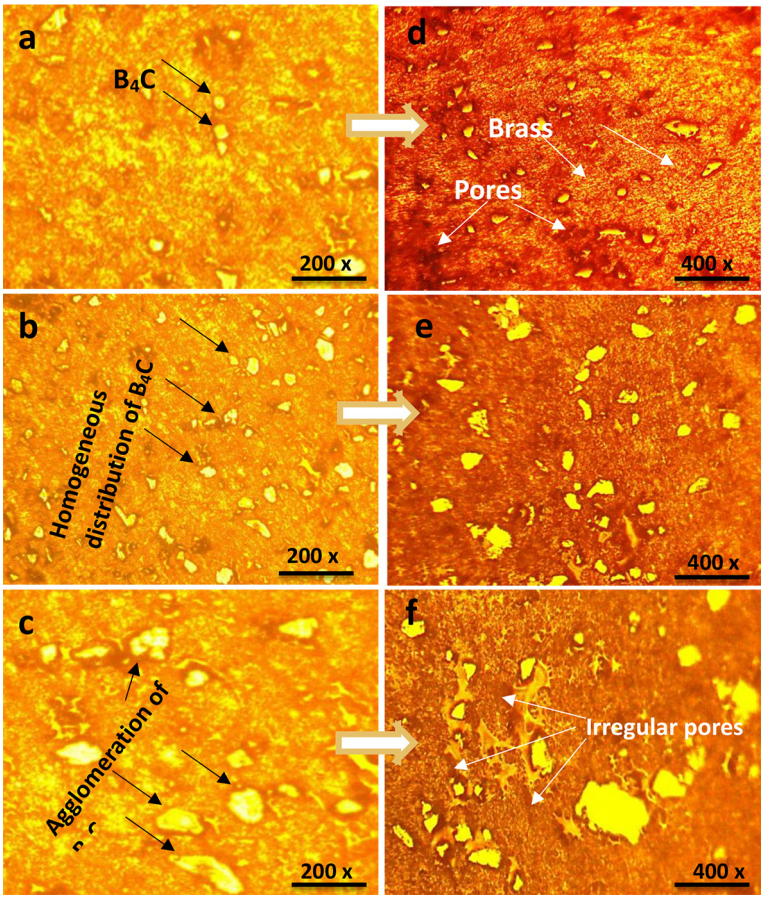


Figure 4. Microstructure of the prepared porous composite: a) S1; b) S5; c) S8 (200× magnification), d) S1; e) S5; f) S8 (400× magnification)

concentration of localised stresses. However, when the reinforcing material is increased to a certain ratio, it agglomerates together, leading to an uneven distribution. This results in stress concentration zones, irregular pores, and cracks adjacent to the agglomerate particles, as shown in Figure 4(c, f). This negatively affects the performance of the composite material. Kargul et al. [3] indicated that a homogeneous distribution of the reinforcing material and the substrate leads to a stable structure and good mechanical properties for composites manufactured using powder metallurgy. Adding 3wt.% B_4C in sample S1(3% B_4C, compacting pressure 600 MPa, sintering temperature 650 °C) results in a homogeneous distribution of reinforcing particles, as shown in Figure 4 (a, d). This is attributed to the low percentage of reinforcing particles, as well as the role of both the compacting pressure and the sintering temperature in achieving structural homogeneity. This interpretation is consistent with studies showing that the distribution quality of the reinforcing material within the matrix is an important factor controlling the mechanical behaviour of composite materials manufactured by powder metallurgy [4, 6]. A recent study by Kelen et al. [5] investigated the formation of a strong bond between the reinforcement and the substrate using hot pressing, and examined its impact on the microstructure and mechanical properties. The addition ratio is increased to 6 wt.% B_4C in sample S5(6% B_4C, compacting pressure 700 MPa, sintering temperature 750 °C), shown in Figure 4 (b, e). This led to a clear improvement in the distribution and homogeneity of the structure. This ratio represented a suitable content of boron carbide particles in the brass substrate. Previous studies on powder metallurgy composites have shown that variations in the reinforcement ratio directly affect the microstructure and mechanical properties [32, 33]. Ansari and Anas [34] explained that a good ratio of reinforcing particles leads to a uniform, homogeneous distribution. Thus, improving the microstructure and mechanical properties. However, when 9 wt.% B_4C in sample S8 (9wt.% B_4C, compacting pressure 700 MPa, sintering temperature 650 °C) was added as shown in Figure 4 (c, f), and agglomeration of

boron carbide particles appeared. This is because the distance between the particles decreases with a high ratio of reinforcing particles, which facilitates their agglomeration during the preparation processes (mixing and pressing). This reduces the efficiency of powder rearrangement during sintering. This results in an inconsistent microstructure and reduced mechanical properties. These results are consistent with Manohar et al [22], who demonstrated that the optimal performance of aluminium composite materials reinforced with boron carbide depends on the homogeneity between the particles and the matrix. Exceeding the acceptable limit leads to the accumulation of particles, resulting in an absence of homogeneity and a decrease in mechanical properties. Similarly, Lateef et al. [35] showed that a homogeneous distribution of reinforcing particles within the aluminium substrate results in a homogeneous structure and good mechanical properties, while heterogeneity leads to different behaviour within the material. The optical microscope provides information about the overall appearance of the microstructure, the distribution of boron carbide particles, and the pores within the substrate. The microstructure results are consistent with the hardness and porosity results, which will be discussed in the next section.

Recent studies confirm that the distribution of reinforcing particles within the metallic substrate is an important factor in the microstructure and mechanical properties of composites. Ansari et al. [36] reported that the manufacturing conditions and ratio of the reinforcing material affect the particle distribution and thus the microstructure, and irregular distribution or aggregation of particles can negatively affect the mechanical properties. This is consistent with current results, where a more homogeneous distribution of B_4C particles was observed at low and medium proportions, while localised clusters appeared when the B_4C content was increased to 9 wt.%. This change in particle distribution can help explain the observed decrease in hardness at higher content.

Furthermore, recent reviews of copper-metal matrix composites have confirmed that the effect of manufacturing conditions on microstructure and mechanical properties is highly dependent on the reinforcement distribution and its interaction with the matrix. This is consistent with the current findings, where changes in B_4C content and manufacturing conditions led to a clear alteration in particle distribution and microstructure, which was reflected in the measured hardness values [37].

Porosity and hardness results

Table 3 shows the experimental design by the Taguchi method (L9), sample code, levels of the affecting parameters, and the porosity and hardness results. The porosity results showed that the highest percentage was 34% for specimen S1 (3% B_4C, compacting pressure 600 MPa, sintering temperature 650 °C), and the lowest was 22% for specimen S8 (9% B_4C, compacting pressure 700 MPa, sintering temperature 650 °C). This indicates the success of urea in producing porosity, which was dissolved before sintering. This difference in porosity between the samples is due not only to urea dissolution but also to manufacturing variables, including the B_4C content, compacting pressure, and sintering temperature used in this study. In sample S1, the high porosity can be attributed to the effect of lower compacting pressure (600 MPa), which reduces the green density and limits the movement of material between the B_4C particles. This encourages a higher percentage of pores to remain in the sintered sample. In the case of sample S8, the use of higher compacting pressure (700 MPa) and a suitable sintering temperature (650 °C) led to an increase in green density and a reorganisation of the particles. This, in turn, improved contact between them, enhancing diffusion and thus reducing porosity. According to previous studies, increasing compacting pressure leads to increased density and reduced interparticle spaces. Furthermore, a higher sintering temperature increases interatomic diffusion and interparticle bonding, which reduces porosity. A study by Tunç et al. [38] showed that increasing pressure and sintering temperature leads to increased density and decreased porosity. Hardness increases as porosity decreases.

As for the hardness results, they ranged from the highest recorded value of 302 HV in sample S5 to the lowest recorded value of 238 HV in sample S4. This is due to the effect of porosity and the proportion of high-hardness B_4C particles, which act as a strengthening phase. The mechanism of the reinforced phase is to impede the movement of dislocations within the brass matrix, thereby increasing its resistance to plastic deformation and increasing the hardness. Furthermore, if the sintering process is successful, the bonding area between the metal particles

and stress concentration around the pores result in higher hardness. On the other hand, increased porosity reduces the surface area subjected to load, leading to stress concentration around the pores. This decreases the embedding resistance during hardness testing. Therefore, it was observed that the samples with high porosity exhibit lower hardness. The hardness increases with improved density, resulting from compacting pressure and sintering efficiency. In addition, increasing the content of boron carbide from 3wt.% B_4C to 6 wt.% B_4C results in increased hardness, reaching the highest value at 6% B_4C. This is attributed to the addition of an appropriate proportion of reinforcing particles, which improves particle distribution within the matrix. During the compacting process, the rearrangement of the powders and the ease of atomic diffusion during the sintering process were enhanced, leading to increased density and homogeneity. This homogeneity allowed the reinforcing particles to contribute to load transfer from the matrix to the particles, thus increasing hardness. Manohar et al. [19] showed that improving hardness and density depends on the distribution of boron carbide particles within the brass matrix. Çanakçı et al. [39] also support the results, as homogenising the powders during mixing leads to a denser, more homogeneous structure.

When increasing the ratio to 9 wt.% B_4C, the hardness decreases. This is due to the accumulation of particles and the beginning of agglomeration, as shown in the microstructure results (Figure 4c). This is because complete condensation does not occur during sintering, and voids remain within the composite material. These act as stress concentration zones, which in turn lead to a decrease in hardness despite the increase in boron carbide particles. Karabacak et al. [40] and Goyal et al. [41] further explained that selecting the appropriate boron carbide particle ratio is crucial for achieving optimal mechanical properties. Manohar et al. [19] stated that exceeding a certain percentage of reinforcing material leads to particle agglomeration, resulting in a heterogeneous structure and reduced mechanical properties. When comparing hardness and porosity, the relationship is inverse: the higher the porosity, the lower the hardness. In this study, hardness was affected not only by porosity but also by the distribution and ratio of B_4C particles within the brass substrate, as well as by the efficiency of the sintering process (Table 3). Therefore, achieving optimal mechanical properties does not depend on a single factor, but rather on the combined effect of several factors, namely the reinforcing material, compacting pressure, and sintering temperature. This was confirmed in the Taguchi and ANOVA analyses in the following section.

Design analysis

Figure 5 shows the main effects plot of process factors on the hardness and porosity. It can be observed that the highest porosity was achieved with a B_4C content of 3%, a compacting pressure of 600 MPa, and a sintering temperature of 650 °C, while the highest hardness was achieved with a B_4C content of 9 wt.%, a compacting pressure of 700 MPa, and a sintering temperature of 650 °C. Figures 6 and 7 show the interaction plot for hardness (HV) and porosity results.

Interaction plots illustrate the combined effect of factors (B_4C content, compacting pressure, and sintering temperature) on both

Table 3. Design of experiments by the Taguchi method (L9), and the porosity and hardness results

Exp. No.	Sample code	Levels of the affecting parameters			Responses	
		B_4C Cxontent (wt.%)	Compacting pressure (MPa)	Sintering temperature (°C)	Hardness (HV)	Porosity (%)
1	S1	3%	600	650	299	34
2	S2	3%	700	700	276	32
3	S3	3%	800	750	248	29
4	S4	6%	600	700	238	25
5	S5	6%	700	750	302	24
6	S6	6%	800	650	242	26
7	S7	9%	600	750	274	28
8	S8	9%	700	650	292	22
9	S9	9%	800	700	283	25

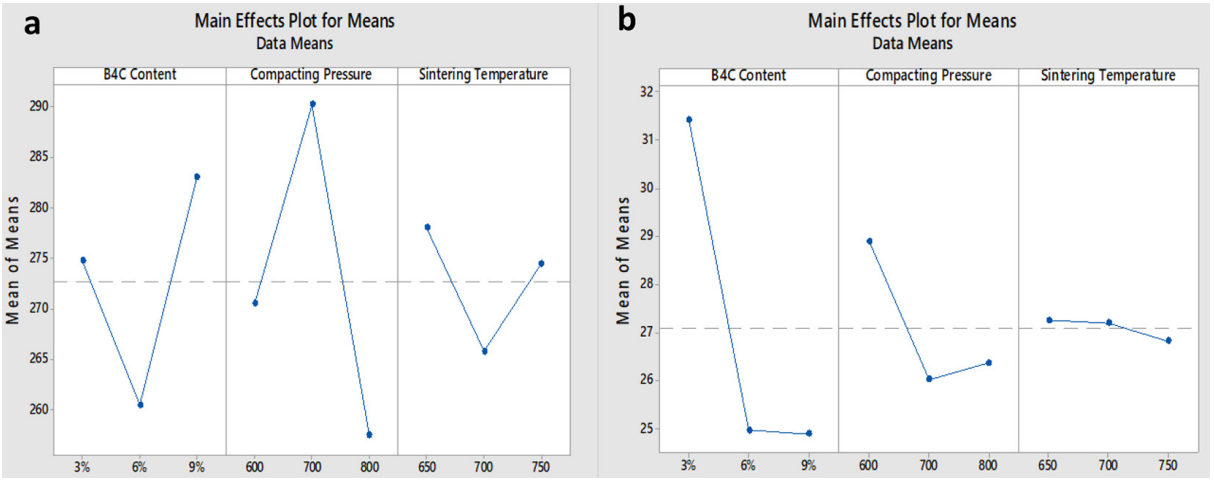


Figure 5. Main effects plot of process factors on a) hardness, b) porosity

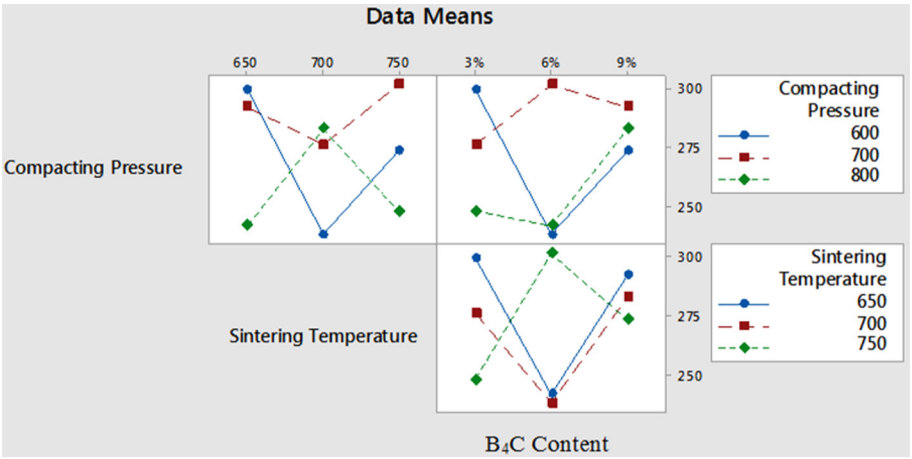


Figure 6. Interaction plot for hardness (Hv) results

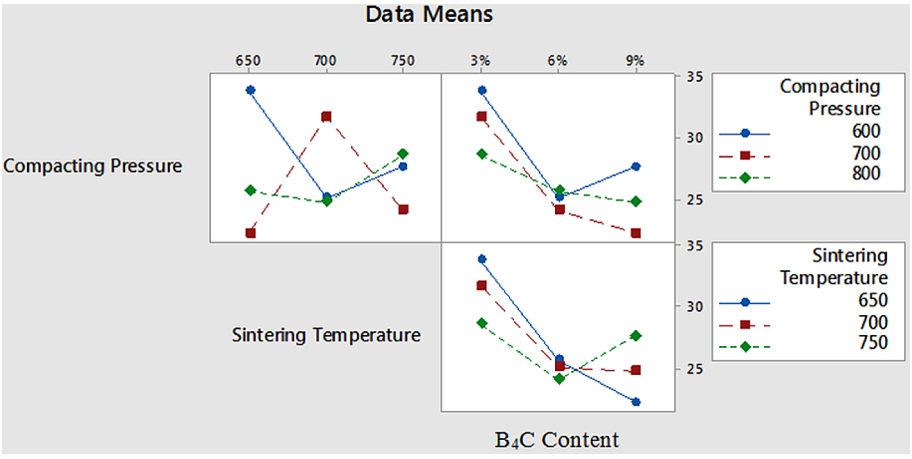


Figure 7. Interaction plot for porosity % results

hardness and porosity. The direction of the lines in these plots indicates the nature of the relationship between the factors used. Close or parallel lines suggest weak or no significant interaction between the factors, while intersecting lines indicate a strong interaction (the effect of one factor depends on the level of the other factors). The results of the signal-to-noise response tables showed that B_4C content ranked first in terms of its effect on porosity and second in terms of

its effect on hardness. Compression pressure ranked first in terms of its effect on hardness and second in terms of its effect on porosity, while the sintering temperature factor ranked third in terms of its effect on both hardness and porosity, as shown in Tables 4 and 5.

Table 6 showed that the p-values for the studied factors exceeded the accepted significance level of 0.05. The results indicated that the effects of the factors did not show statistical significance on the studied responses within the scope of the experiment. The ANOVA analysis also showed the extent to which each factor contributed to the overall variance of responses.

The optimisation plot in Figure 8 is based on the results of the general linear regression model (Equations 2 and 3) used in the ANOVA analysis to determine the levels of factors that achieve the best performance for the studied responses.

The optimisation results showed that the composite desirability value reached 0.8, a good value indicating that the proposed optimal levels achieve good alignment between the response objectives. As for the individual responses, the desirability value for porosity was 0.7 and for hardness 0.9, indicating that an acceptable level of the desired objective was achieved.

$$\begin{aligned} &Hardness\ (Hv) = \\ &= 272.7 + 1.7\ B_4C\ content\ (3\ wt.\%) \\ &- 12.0\ B_4C\ content\ (6\ wt.\%) \\ &+ 10.3\ B_4C\ content\ (9\ wt.\%) \\ &- 2.3\ compacting\ pressure\ (600\ MPa) \\ &+ 17.3\ compacting\ pressure\ (700\ MPa) \\ &- 15.0\ compacting\ pressure\ (800\ MPa) \\ &+ 5.0\ sintering\ temperature\ (650\ °C) \\ &- 7.0\ sintering\ temperature\ (700\ °C) \\ &+ 2.0\ sintering\ temperature\ (750\ °C) \end{aligned} \quad (2)$$

Table 4. Response table for signal- to- noise ratios for hardness

Level	B_4C %	Compacting pressure (MPa)	Sintering temperature (ºC)
1	48.74	48.60	48.83
2	48.27	49.24	48.46
3	49.03	48.20	48.75
Delta	0.76	1.04	0.37
Rank	2	1	3

Table 5. Response table for signal- to- noise ratios for porosity

Level	B4C %	Compacting pressure (MPa)	Sintering temperature (ºC)
1	29.99	29.18	28.59
2	27.95	28.19	28.67
3	27.92	28.50	28.60
Delta	2.08	0.99	0.08
Rank	1	2	3

Table 6. Analysis of variance for individual responses of hardness and porosity

Parameter	Source	DF	Adj SS	Adj MS	F-Value	P-Value	Contribution (%)
Hardness	B_4C content wt%	2	760.7	380.3	0.34	0.744	15.85%
	Compacting pressure (MPa)	2	1592.7	796.3	0.72	0.581	33.19%
	Sintering temperature (˚C)	2	234.0	117.0	0.11	0.904	4.87%
	Error	2	2210.7	1105.3			–
	Total	8	4798.0				–
Porosity	B_4C content wt%	2	88.889	44.4444	5.06	0.165	73.12%
	Compacting pressure (MPa)	2	14.889	7.4444	0.85	0.541	12.24%
	Sintering temperature (˚C)	2	0.222	0.1111	0.01	0.988	0.18%
	Error	2	17.556	8.7778			–
	Total	8	121.556				–

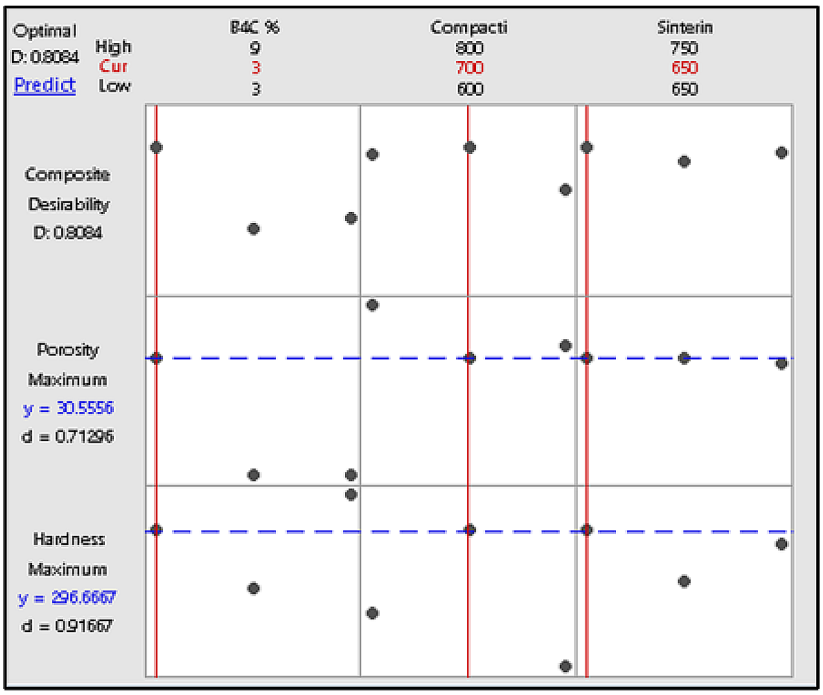


Figure 8. Optimisation results

Table 7. Results of confirmation test

Response variables	Optimal conditions		Error %
	Predicted	Experimental	
Level	B_4C (3%) Compacting pressure (700 MPa), sintering temperature (650 °C)	B_4C (3%) Compacting pressure (700 MPa), sintering temperature (650 °C)	
Hardness (Hv)	296.7	297	0.10%
Porosity (%)	30.56	30.98	1.37%

$$
\begin{aligned}
Porosity = \\
&= 27.222 + 4.44\ B_4C\ content\ (3\ wt.\%) \\
&- 2.22\ B_4C\ content\ (6\ wt.\%) \\
&- 2.22\ B_4C\ content\ (9\ wt.\%) \\
&+ 1.78\ compacting\ pressure\ (600\ MPa) \\
&- 1.22\ compacting\ pressure\ (700\ MPa) \\
&- 0.56\ compacting\ pressure\ (800\ MPa) \\
&+ 0.11\ sintering\ temperature\ (650\ °C) \\
&+ 0.11\ sintering\ temperature\ (700\ °C) \\
&- 0.22\ sintering\ temperature\ (750\ °C) \quad (3)
\end{aligned}
$$

The plot shows the expected values for the responses at the optimal levels (3% B_4C, pressure 700 MPa, and sintering temperature 650 °C), which represent the expected performance according to the model. These optimal levels were used to conduct the confirmation test, and the test results presented in Table 7 show agreement between the experimental and predicted results, supporting the possibility of using the model to predict responses under the study conditions.

CONCLUSIONS

The scientific novelty of this study lies not only in the preparation of a porous brass compound, but also in the development of these porous brass compounds with improved mechanical properties using powder metallurgy methods and under various manufacturing conditions. Brass (70% Cu, 30% Zn) was reinforced with 3, 6, and 9 Wt.% of boron carbide. To create the pores, spherical urea granules (diameter approximately 425 µm) were used as a space holder at a weight percentage of 30%. The powders were compacted at three different pressures: 600, 700, and 800 MPa. The specimens were sintered at temperatures of 650, 700, and 750 °C for 120 min under a vacuum atmosphere of 10^{-4} torr. In addition, the use of statistical optimisation allowed for an understanding of the effect of manufacturing conditions on controlling porosity and hardness

and producing compounds with better properties. This could be used to design porous brass composites for use in engineering applications, thus bridging the gap shown by previous studies.

1. The apparent porosity was directly affected by the fabrication conditions. The results showed apparent porosity of 22% to 34%. Higher compression pressure and sintering temperature led to a decrease in porosity due to improved condensation and increased interparticle bonding.
2. Micro-hardness increased from 238 HV to 302 HV with improved sintering conditions and decreased porosity. The addition of B_4C particles also improved the material's deformation resistance due to their high hardness and matrix reinforcement.
3. The microstructure showed an acceptable distribution of B_4C particles within the brass matrix, with pores appearing after urea removal, confirming the success of the powder metallurgy fabrication process.
4. The results of the signal-to-noise ratio analysis and main effects plots showed a difference in the effect of factor levels on response performance, which helped in identifying suitable conditions.
5. The optimisation plot results showed that the desirability value was good, indicating that the proposed optimal conditions achieve a good balance between the different responses.

REFERENCES

1. Goyal B., Pandey A. Critical review on porous material manufacturing techniques, properties & their applications. Mater. Today Proc. 2021; 46: 8196–8203.
2. Mutuk T., Akyol Ö. Synergistic effects of B_4C and graphite on the multifunctional properties of copper-based hybrid composites. Diam. Relat. Mater. 2025; 160: 112996. https://doi.org/10.1016/j.diamond.2025.112996
3. Kargul M. Influence of the type of strengthening particles on the tribological and material properties of sintered copper matrix composites. Adv. Sci. Technol. Res. J. 2025; 19(9): 19–33. https://doi.org/10.12913/22998624/205674
4. Aydoğmuş T, Al-Zangana NJF, Kelen F. Processing of β-type biomedical Ti74Nb26 alloy by combination of hot pressing and high-temperature sintering. Konya J. Eng. Sci. 2020; 8(2): 269–281. https://doi.org/10.36306/konjes.587790
5. Kelen F. Assessing microstructural and mechanical characteristics of Ni/AZ91 composites manufactured using hot pressing technique for automotive applications. Mater. Chem. Phys. 2025; 339: 130793. https://doi.org/10.1016/j.matchemphys.2025.130793
6. Kelen F. Novel magnesium matrix hybrid composites manufactured through powder metallurgy technique. Mater. Today Commun. 2023; 35: 106348. https://doi.org/10.1016/j.mtcomm.2023.106348
7. Rodriguez-Contreras A., Punset M., Calero J.A., Gil F.J., Ruperez E., Manero J.M. Powder metallurgy with space holder for porous titanium implants: A review. J. Mater. Sci. Technol. 2021; 76: 129–149. https://doi.org/10.1016/j.jmst.2020.11.005
8. Zhang L., Shi J., Shen C., Zhou X., Peng S., Long X. B4C-Al composites fabricated by the powder metallurgy process. Appl. Sci. 2017; 7(10): 1009. https://doi.org/10.3390/app7101009
9. Stavroulakis P., Toulfatzis A.I., Pantazopoulos G.A., Paipetis A.S. Machinable leaded and eco-friendly brass alloys for high-performance manufacturing processes: A critical review. Metals 2022; 12(2): 246. https://doi.org/10.3390/met12020246
10. Jasper S., Subash R., Muthuneelakandan K., Vijayakumar D., Jhansi Ida S. The mechanical properties of brass alloys: A review. Eng. Proc. 2025; 93(1): 11. https://doi.org/10.3390/engproc2025093011
11. Kaytarov Z., Burnashev V., Fayziev B., Alwadood Z., Jumayev A., Khaydarov O., Namazov G.A. Numerical investigation of the multiphase filtration process considering medium and phase compressibility. Eng. Technol. Appl. Sci. Res. 2026; 16(1): 30787–30794. https://doi.org/10.48084/etasr.14097
12. Aminnudin A., Suryanto H., Ghazali C.M.R., Setiawan D.D. Enhancing wear resistance of brass composites using fly ash reinforcement: A specific weight loss study. Eng. Technol. Appl. Sci. Res. 2026; 16(1): 30822–30828. https://doi.org/10.48084/etasr.13243
13. Zhang W. A review of tribological properties for boron carbide ceramics. Prog. Mater. Sci. 2021; 116: 100718. https://doi.org/10.1016/j.pmatsci.2020.100718
14. Dyatkin B., Laskoski III M., Edelen W.K., Qadri S.B., Keller T.M. Synthesis, structure, and properties of polymer-derived, metal-reinforced boron carbide cermet composites. Int. J. Appl. Ceram. Technol. 2021; 18(2): 457–471. https://doi.org/10.1111/ijac.13657
15. Stanev L.M., Kolev M., Drenchev B., Drenchev L. Open-cell metallic porous materials obtained through space holders—Part I: Production methods. A review. J. Manuf. Sci. Eng. 2017; 139(5): 050801. https://doi.org/10.1115/1.4034439
16. Zhao B., Gain A.K., Ding W., Zhang L., Li X., Fu Y. A review on metallic porous materials: Pore formation, mechanical properties, and their applications.

Int. J. Adv. Manuf. Technol. 2018; 95: 2641–2659. https://doi.org/10.1007/s00170-017-1415-6

17. Abdullah Z., Ahmad S., Ramli M. The impact of composition and sintering temperature for stainless steel foams (SS316L) fabricated by space holder method with urea as space holder. Mater. Sci. Forum 2017; 888: 413–417. https://doi.org/10.4028/www.scientific.net/MSF.888.413
18. Batool H., Shen J., Long X. Advancements in metallic foams for high-performance applications: Energy absorption and lightweight materials. Adv. Compos. Hybrid Mater. 2026; 9: 209. https://doi.org/10.1007/s42114-026-01726-6.
19. Manohar G., Pandey K.M., Maity S.R. Characterization of boron carbide (B_4C) particle reinforced aluminum metal matrix composites fabricated by powder metallurgy techniques – A review. Mater. Today Proc. 2021; 45: 6882–6888. https://doi.org/10.1016/j.matpr.2020.12.1087
20. Xiao Y., He Y., Ma W., Yue Y., Qiu G. Effects of the space holder shape on the pore structure and mechanical properties of porous Cu with a wide porosity range. Materials 2024; 17(12): 3008. https://doi.org/10.3390/ma17123008
21. Fujii T., Saito T., Shimamura Y. Fabrication of porous steels via space holder technique and their mechanical properties. Mater. Trans. 2023; 64(7).
22. Lascano S., Amigó C., Montealegre-Meléndez I., Muñoz S., Rodríguez-Ortiz J.A., Torres Y. Porous titanium for biomedical applications: Evaluation of the conventional powder metallurgy frontier and space-holder technique. Appl. Sci. 2019; 9(5): 982. https://doi.org/10.3390/app9050982
23. Aydoğmuş T, Palani DKH, Kelen F. Processing of porous β-type Ti74Nb26 alloys for biomedical applications. J. Alloys Compd. 2021; 872: 159737. https://doi.org/10.1016/j.jallcom.2021.159737
24. Lee D.J., Jung J.M., Jeong J., Oh S.H., Lee C.S., Kim H.S. Effect of microstructure on the tensile property of porous Ti produced by powder metallurgy technique. Mater. Sci. Eng. A 2012; 534: 43–52. https://doi.org/10.1016/j.msea.2011.11.028
25. Sharma M., Gupta G.K., Modi O.P., Prasad B.K. PM processed titanium foam: Influence of morphology and content of space holder on microstructure and mechanical properties. Powder Metall. 2013; 56(1): 55–60. https://doi.org/10.1179/1743290112Y.0000000036
26. Jain H., Gupta G., Kumar R., Mondal D.P. Microstructure and compressive deformation behavior of SS foam made through evaporation of urea as space holder. Mater. Chem. Phys. 2019; 223: 737–744. https://doi.org/10.1016/j.matchemphys.2018.11.040
27. Čákyová V., Gorejová R., Macko R., Petruš O., Sopčák T., Kupková M., Kaľavský F., Oriňáková R. Biodegradable iron-based foams prepared by the space holder technique using urea. J. Appl. Electrochem. 2024; 54: 625–634. https://doi.org/10.1007/s10800-023-01993-x
28. He Y., Xiao J., Xie S., Tan R., Qiu G. Effects of the space holder size on the pore structure and mechanical properties of porous Cu with a wide porosity range. Scientific Reports. 2025; 15:11072. https://doi.org/10.1038/s41598-025-87570-y
29. Moradi M.R., Moloodi A., Habibolahzadeh A. Fabrication of nano-composite Al–B_4C foam via powder metallurgy-space holder technique. Procedia Mater. Sci. 2015; 11: 553–559. https://doi.org/10.1016/j.mspro.2015.11.059
30. ASTM International. Standard Practice for Microetching Metals and Alloys. ASTM E407-07(2015). West Conshohocken, PA, USA: ASTM International; 2015.
31. Fooladi S., Ashrafizadeh F., Golozar M.A., Razavi S.A. Influence of age hardening on mechanical properties of cast nickel-aluminum bronze containing shrinkage porosity. J. Fail. Anal. Prev. 2019; 19(5): 1498–1508. https://doi.org/10.1007/s11668-019-00757-0
32. Kelen F, Gavgali M, Aydoğmuş T. Microstructure and mechanical properties of a novel TiNi particulate-reinforced AZ91 metal matrix composite. Mater. Lett. 2018; 233: 12–15. https://doi.org/10.1016/j.matlet.2018.08.121
33. Kelen F. Processing and characterization of magnesium matrix composites reinforced by nickel particles. Afyon Kocatepe Univ. J. Sci. Eng. 2023; 23(5): 1318–1327. https://doi.org/10.35414/akufemubid.1207488
34. Ansari, A.J., Anas, M. Effect of volume percentage of reinforcement on the microstructure and mechanical properties of an Al6061-T6/SiC surface composite fabricated through friction stir processing. Adv. Sci. Technol. Res. J., 2023; 17(2): 247–257. https://doi.org/10.12913/22998624/161690
35. Lateef, H., Aghdeab, S.H., Mahdi, B.S. (2023). Investigation of adding microscopic slide glass nanoparticles on the metallurgical characterization and mechanical properties of cast aluminum 7075 composites. Adv. Sci. Technol. Res. J., 17(3): 214–225. https://doi.org/10.12913/22998624/166282
36. Ansari AJ, Ansari S, Alam N. Fabrication of aluminium surface composites synthesized through friction stir processing: Optimization of process parameters through response surface methodology. J. Eng. Sci. Technol. Rev. 2025; 18(5): 218–230. https://doi.org/10.25103/jestr.185.21
37. Ansari AJ, Mahto MK, Yadav AP, Tiwari K. Research status and development trends of copper metal matrix composites synthesized through friction stir processing: An analysis of process parameters.

Trans. Indian Inst. Met. 2025; 78(7). https://doi.org/10.1007/s12666-025-03657-0

38. Tunç S.A., Çanakçı A., Karabacak A.H., Çelebi M., Türkmen M. Effect of different PCA types on morphology, physical, thermal and mechanical properties of AA2024-B_4C composites. Powder Technol. 2024; 434: 119373. https://doi.org/10.1016/j.powtec.2024.119373
39. Çanakçı A., Karabacak A.H., Çelebi M., et al. A study on the optimization of nano-B_4C content for the best wear and corrosion properties of the Al-based hybrid nanocomposites. Arab. J. Sci. Eng. 2024; 49: 14625–14641. https://doi.org/10.1007/s13369-024-08736-w
40. Tunç S.A., Çanakçı A., Karabacak A.H., Çelebi M., Türkmen M. Effect of different PCA types on morphology, physical, thermal and mechanical properties of AA2024-B_4C composites. Powder Technol. 2024; 434: 119373. https://doi.org/10.1016/j.powtec.2024.119373
41. Goyal A.K., Pandey K.M. Recent developments in powder metallurgy processed B_4C-reinforced metal matrix composites: A review. Mater. Today Proc. 2021; 44: 4389–4395.